Fast optical vapour sensing by Bloch surface waves on porous silicon membranes

Francesco Michelotti,†*[a] Beniamino Sciacca,[b] Lorenzo Dominici,[c] Marzia Quaglio,[b] Emiliano Descrovi,[b] Fabrizio Giorgis†[b] and Francesco Geobaldo[b]

Received 16th July 2009, Accepted 17th September 2009
First published as an Advance Article on the web 16th November 2009
DOI: 10.1039/b914280k

The coupling of optical Bloch surface waves at the truncated end of one dimensional porous silicon photonic crystals is exploited for fast vapour sensing. Self-standing multilayered membranes bound to transparent substrates were fabricated by electrochemical etching and used in an attenuated total reflection configuration to resonantly excite the surface waves and perform real-time sensing.

Porous silicon (PS) was proposed for vapour sensing in 1990 by Anderson *et al.*[1] Among other types (electrical, electrochemical, ...), various optical PS sensors were reported based on spectroscopic ellipsometry,[2] Fabry–Perot resonance in single layers,[3] Bragg mirrors,[4] microcavities,[5,6] and resonant tunneling in superlattices.[7] Recently, Guillermain *et al.* reported on optical biosensors exploiting the excitation of surface electromagnetic waves, also called Bloch surface waves (BSW), at the truncated end of a one-dimensional photonic crystal (1DPC) made of porous silicon.[8] BSW in 1DPC were originally introduced by Yeh *et al.*,[9] and during the last years have been the object of an increasing number of papers,[10–12] highlighting their extremely appealing features for sensing applications and as an efficient alternative to surface plasmon resonance (SPR).[13]

In earlier work, we reported on vapour sensing by BSWs, excited by attenuated total reflection (ATR) in the Otto configuration, at the surface of PS-1DPC at $\lambda \in [1450, 1590\ \text{nm}]$.[14] The 1DPC was fabricated by electrochemical etching onto 300 μm-thick p^+ silicon wafers.[15] We demonstrated that the large PS effective surface area associated with the extremely narrow BSW resonances (BSWR) leads to an enhanced sensitivity to ethanol. In ATR, the exponential tail of the excitation beam, that is totally reflected at the prism base, is resonantly coupled to the BSW. In ref. 8 and 14, the use of the Otto configuration, as sketched in Fig. 1(a), was imposed by the fact that either bound or free carriers are strongly absorbing in the VIS-NIR and do not permit propagation of light in thick p^+ substrates. Therefore, the PS-1DPC top surface had to be in a direct, close proximity to the prism surface. Working in the Otto configuration leads to two major drawbacks. First of all, BSWs coupling efficiency critically depends of the width of the air gap between the prism and the PS-1DPC surface and must be optimised by accurately controlling the mechanical force applied to the prism.[14] Second, and more important, the coupling prism screens the PS-1DPC surface and the sensor response time is detrimentally increased ($\tau \sim 10$ min),[14] as the vapours must flow through the air gap before penetrating within the pores of the PS-1DPC.

In the present work, we report on the design, fabrication and characterization of vapour sensors based on PS membranes with a very fast rise and fall time.

PS-1DPC were prepared from single polished (100)-oriented Boron-doped p^+-type silicon wafers (<7 mΩ cm resistivity) by calibrated[15] electrochemical etching in a HF/35%H_2O/35%EtOH/30% solution. The silicon wafers were previously treated in air at 300 °C for 2 h, in order to depassivate the Boron atoms underlying the surface from H, which can lead to the formation of a parasitic surface film that is detrimental for

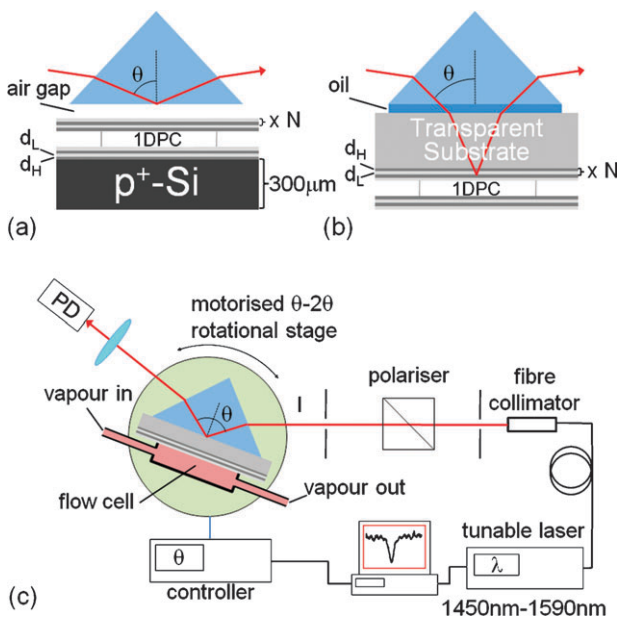

Fig. 1 Sketch of the (a) Otto and (b) Kretschmann configurations used in ATR experiments. In the first case the laser beam is totally reflected at the prism base, in the second case the beam is reflected by the Bragg mirror in the stop band. (c) Setup for ATR measurements.

[a] *SAPIENZA Università di Roma, Dipartimento di Energetica, Via A.Scarpa, 16 00161 Roma, Italy. E-mail: francesco.michelotti@uniroma1.it; Tel: +39-06-49.91.65.62*
[b] *Politecnico di Torino, Dipartimento di Scienza dei Materiali e Ingegneria Chimica, Torino, Italy*
[c] *Università degli Studi di Roma "Tor Vergata", CHOSE- Centre for Hybrid and Organic Solar Energy, Roma, Italy*
† F. Michelotti and F. Giorgis are also with Consorzio Nazionale Interuniversitario per le Scienze Fisiche della Materia (CNISM).

the optical quality of porous silicon samples. A HF rinse in a HF/20%H_2O/20%EtOH/60% solution was performed for 5 min before the etch to remove the thin oxide layer formed during the depassivation; the chip was then rinsed several times with ethanol and dried under a flow of Argon.

The etching process was performed by means of a source-meter (Keithley 2630), in a Teflon cell with a platinum electrode. The etching temperature was −25 °C in order to have smoother interfaces between the layers and a better control of their refractive index and thickness. PS-1DPC were obtained through a pseudo-periodical current waveform varying between 12.7 and 19 mA cm^{-2}, applied for N cycles (22 s for each cycle). An etch stop (10 s) was applied to ensure the best in-depth homogeneity of the porous layers. The fabricated 1DPC were constituted by N periods of high (H) and low (L) refractive index layers characterized by the following thicknesses and porosities: d_H = 215 nm, p_H = 49% and d_L = 240 nm, p_L = 58%, respectively. At λ = 1530 nm, the refractive indices are, respectively, n_H = 2.15 and n_L = 1.89. We consider several layouts, with the number of periods, N, ranging from 10 to 25. The PS-1DPC were designed with a low refractive index first layer (high porosity) in order to sustain TE-polarised BSW.

After fabricating the 1DPC, we etched a thick buffer layer to decrease the brittleness of the final membranes. The layer was etched at 35 mA cm^{-2} for 430–550 s (depending on N) under the same conditions. The layer porosity and refractive index were p_B = 68%, n_B = 1.61, respectively.

The membranes (1DPC and buffer layer), with a total thickness L = 37 μm, were subsequently detached from the bulk Si by applying a current of 190 mA cm^{-2} for 21 s in a HF/35%H_2O/35%EtOH/30% solution at −25 °C, using the electropolishing reaction.[15] They were then gently rinsed several times with ethanol, dried under a stream of Argon, and eventually placed onto soda lime microscope slides (Menzel–Glaser extra white glass, n_S = 1.517) previously coated with a AZ5214E (Clariant) photoresist layer. They were positioned so that the 1DPC side was free to be exposed to target vapours. The glass slides were then placed on a hot plate and heated up to 110 °C in air for 5 min, in order to allow the evaporation of the residual solvent in the photoresist and to promote the creation of a polymeric bonding layer between the membrane and the glass. To increase the strength of the bonding interfaces generated by heating, a force is applied to the membrane to keep it in perfect contact against the glass slide. The applied force is normal to the membrane surface. The resulting applied stress must be uniform, to avoid fractures and defects into the membrane. A second glass slide was placed over the membrane, without any polymeric film, to distribute the load uniformly.

The final integrated structures, bearing the stratified membranes, were mounted on the BK7 coupling prism (n_p = 1.501) of our ATR experimental set-up in the so called Kretschmann configuration, as sketched in Fig. 1(b), that is currently used for both metal layers (SPR) and 1DPC with transparent substrates (BSWR).[13,16] The back face of the sensor is in contact with the prism facet by means of an index matching oil (n_o = 1.66). The transparency of the glass substrate, the limited thickness of the buffer layer and its porosity make the absorption losses low. The impinging laser beam can therefore tunnel through the PS-1DPC and efficiently excite the BSW at the free PS-1DPC/air truncation interface.

In Fig. 1(c), the experimental set-up is shown. A collimated and TE-polarized beam is expanded from a fibered, tunable diode laser source (Nettest, Tunics-Plus) and used to illuminate the sample through the prism. θ is the angle between the normal to the prism base and the direction of the incident beam inside the prism. A lens focuses the reflected light onto the photodiode (PD). Reflectance profiles at fixed wavelengths were obtained by rotating the prism and the photodiode with respect to the incident beam in a θ–2θ configuration. The PS-1DPC is topped by a flow cell, with volume V_0 = 1.4 cm^3, used in the vapour sensing experiments and contacted to the surface by means of an o-ring.

As an example, in Fig. 2(a) we show the experimental reflectance map $R(\theta,\lambda)$, measured as a function of θ and of the wavelength λ, obtained in air environment for a sensor having N = 12. Dark regions correspond to low reflectance. The vertical line at $\theta \sim 42^\circ$ is the total internal reflection angle (air light line). The dispersion of the BSW appears as a narrow line laying beyond the air light line. The weak fringe pattern appearing in background is due to interference in the thick buffer layer. A guided mode, propagating in the bulk of the 1DPC is also observed corresponding to a broader line broken by the interference pattern. For the sake of clarity, in the inset of Fig. 2(a), we show the result of a measurement of $R(\lambda)$ obtained at fixed θ = 58.37°, in which the BSW appears as a Lorentzian-shaped resonance. At the minimum, R is decreased by 46% and the width of the resonance is $\Delta\lambda_{FWHM}$ = 7.3 nm. The $\Delta\lambda_{FWHM}$ value is larger than the value we observed for a PS-1DPC with N = 25 in the Otto configuration ($\Delta\lambda_{FWHM}$ = 5.1 nm).[14] The main reason is that, in the present case, coupling (that in the Kretschmann is basically controlled by the number of periods, N)[17] is stronger and gives rise to a broadening in ATR.[18]

In order to narrow the linewidth and increase the sensitivity in vapour sensing, we decided to operate with PS-1DPC with larger N. Therefore, in the following we shall report experiments obtained for PS-1DPCs with N = 25. The drawback is that the resonance is less pronounced.

The response of the sensor was tested with respect to exposure to saturated vapours extracted from reservoirs partially filled with different alcohols in equilibrium at ambient temperature, T_{amb} = 25 °C and vapour pressure, p_0. We used methanol, ethanol and 2-propanol. In a typical experiment, the sensor is fixed at a particular angle (θ_0 = 50.66°) such that the BSWR is observed at λ_0 = 1480 nm. With reference to the experimental measurement reported in Fig. 2(b) obtained for ethanol, $R(\lambda)$ is recorded every Δt in a convenient spectral range including λ_0. Values of Δt are different for each species and are reported in Table 1. In the inset of Fig. 2(b), we also show the reflectance spectrum around λ_0 at time zero. Due to the larger number of periods (N = 25) the resonance is only 14% deep but $\Delta\lambda_{FWHM}$ = 4.9 nm, indicating a better sensitivity with respect to the case of Fig. 2(a) (N = 12).

At the beginning, the flow cell is full of laboratory air. At a given time, the vapour is filled in and the input and output hoses are subsequently closed, therefore realizing non-stationary

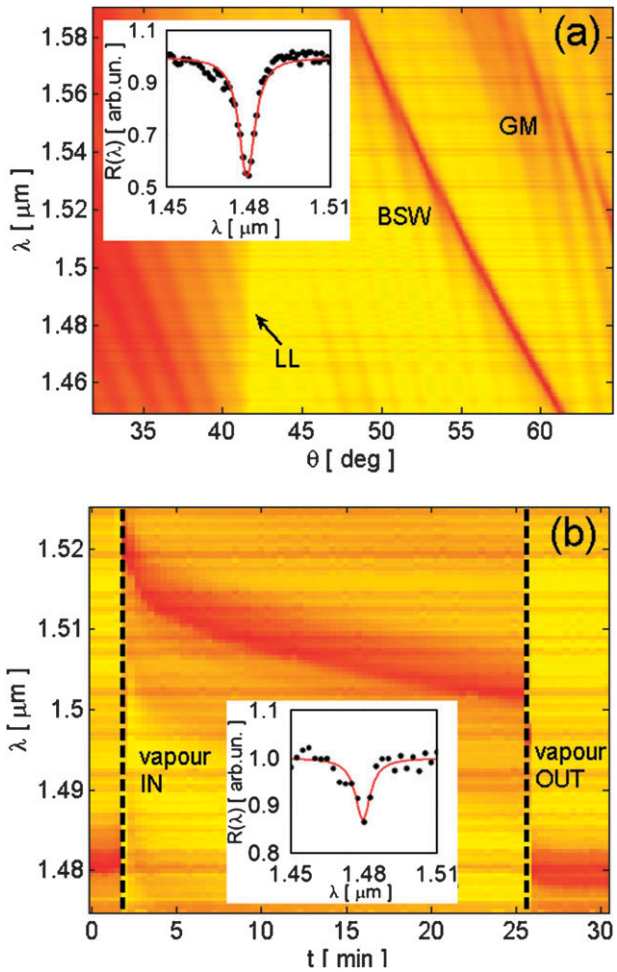

Fig. 2 (a) Experimental ATR map, $R(\theta,\lambda)$, obtained in the window $\theta \in [32, 67^\circ]$ and $\lambda \in [1.45, 1.59\ \mu m]$ for a PS-1DPC with $N = 12$ periods. The BSW dispersion appears as a line in the map beyond the light line (LL). A mode guided in the bulk of the multilayer (GM) is also observed. Inset: spectral reflectance at fixed angle $\theta = 58.37^\circ$, at the resonance, R, is reduced to 46% and the $\Delta\lambda_{FWHM} = 7.1$ nm. (b) Time resolved spectral reflectance measurements, $R(\theta_0,\lambda)$, obtained in the window $\lambda \in [1.47, 1.59\ \mu m]$ at $\theta_0 = 50.66^\circ$ for a PS-1DPC with $N = 25$ periods. The BSWR suddenly shifts by $\Delta\lambda_{MAX,EXP}$ when exposing the sensor to ethanol vapours at pressure p_0 at 25 °C. A biexponential decay is observed afterwards. The BSWR resonance recovers its position if the vapour is pumped out from the flow cell and laboratory air is allowed back in again. Inset: spectral reflectance at fixed angle $\theta_0 = 50.66^\circ$, at the resonance, R, is reduced to 14% and the $\Delta\lambda_{FWHM} = 4.9$ nm.

measurement conditions. A steep red-shift of the position of the resonance dip, followed by a slow decay towards the original position, λ_0, are observed. When the vapour is completely pumped out and the flow cell is filled with the environmental air again, we observe a steep shift back to the original position of the BSWR at λ_0. The same behavior was observed after performing any number of cycles, therefore demonstrating the complete reversibility of the sensor response.

The slight deviation of the BSWR with respect to its original position is due to a thermal change of the refractive indices originating from the cooling during the liquid/vapour transition taking place inside the porous silicon 1DPC structure. This effect is larger for 2-propanol, which is characterized by a larger value of the enthalpy of vaporization. In any case, we experimentally verified that, after a thermalisation time, the BSWR returns to the original position.

In Fig. 3, we report the dynamic behavior of the BSWR wavelength, λ_{BSWR}, as a function of time for methanol (circles), ethanol (squares) and 2-propanol (diamonds). At the present stage, the three standard compounds were chosen as a minimum set, characterized by different physical chemical properties, with the aim to provide an insight into the diffusion dynamics rather than to test the selectivity. The curves were extracted from measurements similar to that shown in Fig. 2(b). The extremely large and steep initial red-shift of λ_{BSWR}, taking place on a timescale shorter than Δt, indicates that the BSW is sensing the capillary condensation of the vapour at the surface of the PS-1DPC at very early times after exposure. The response time appears much shorter than those observed, for example, in PS microcavities, whose sensitive layer is buried inside the multilayer structure.[19] We point out that capillary condensation must necessarily take place because the refractive index of the vapour, under any conditions, could not perturb the structure to such an extent to justify the observed shifts.

The slow decays observed in Fig. 2(b) and 3 suggest that a second process is taking place after the rapid condensation and the establishment of a new equilibrium between the liquid in the PS structures and the vapour in the cell at a pressure $p < p_0$. We attribute this decay to a diffusion of the condensed liquid inside the porous structure, starting from the initial conditions, in which the liquid is within a superficial layer only. In fact, given that the sensing mechanism is transduced by a BSW, that is mostly confined at the surface, the perturbation and the resulting red-shift of the resonance tend to decrease as the liquid is leaving the surface when diffusing in depth. We

Table 1 Values of all parameters used for the three alcohols used in the experiments: Δt is the temporal resolution in the spectral sensing experiments; p_0, m_v, ρ, and n are respectively the vapour pressure at 25 °C, the mass of vapour before condensation inside the 1.4 cm^3 flow cell, the density and the refractive index in the liquid phase; h_{MAX} is the maximum thickness of the condensed liquid layer resulting from the assumption that all vapour in the cell is condensing; $\Delta\lambda_{MAX,TH}$ is the resulting maximum shift of the BSWR; $\Delta\lambda_{MAX,EXP}$ is the measured shift of the BSWR under non stationary conditions; τ_S and τ_L are the two time constants of the biexponential decays shown in Fig. 3; k is the diffusion constant measured from τ_S and appearing in eqn (1)

Vapour	Δt/s	p_0[a]/kPa	m_V/μg (n_V/μ mol)	ρ/g cm^{-3}	n	h_{MAX}/μm	$\Delta\lambda_{MAX,TH}$ ($\Delta\lambda_{MAX,EXP}$)/nm	τ_S/min	τ_L/min	k/m^2 s^{-1}
methanol	28.0	16.20	293 (9.1)	0.792	1.33	8.8	240 (56.3)	0.6 ± 0.1	24.4 ± 0.8	9.9 ± 0.3
ethanol	23.0	7.54	196 (4.3)	0.789	1.36	5.8	258 (39.8)	1.14 ± 0.07	33 ± 3	6.9 ± 0.6
2-propanol	34.5	5.87	199 (3.3)	0.786	1.38	6.0	272 (66.4)	1.09 ± 0.05	52 ± 3	4.4 ± 0.3

[a] at $T_{amb} = 25$ °C

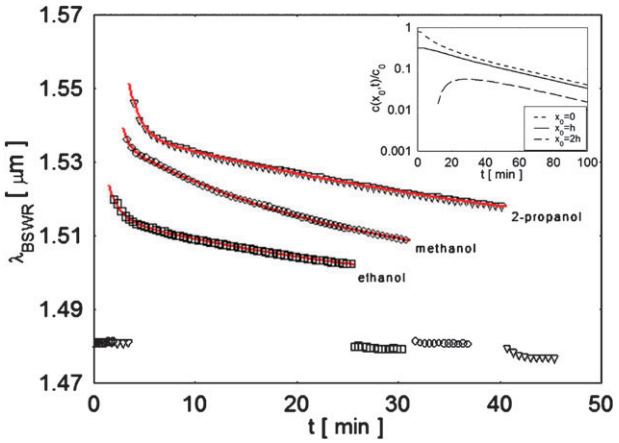

Fig. 3 Experimental measurements of the position of the BSWR as a function of time obtained when PS-1DPCs with $N = 25$ are exposed to methanol (circles), ethanol (squares), and 2-propanol (diamonds). The curves were extracted by measurements similar to that shown in Fig. 2(b). The solid red curves are fits with biexponential functions with time constants τ_S and τ_L values reported in Table 1. Inset: calculated temporal dependence of the normalized concentration inside the PS-1DPC at three different depths inside the structure: (dashed) $x_0 = 0$, (solid) $x_0 = h_0$ and (long dashed) $x_0 = 2h_0$.

point out that such a phenomenon can be observed as the measurement is performed in non-stationary conditions and the amount of alcohol in the flow cell is fixed. The temporal decays shown in Fig. 3 can be fitted by a double exponential curve characterized by a short (τ_S) and a long (τ_L) time constant. Fitted values are reported in Table 1.

Even assuming that all the vapour in the flow cell condenses uniformly inside the PS-1DPC in the proximity of its exposed surface, we evaluate that the liquid would occupy the sensor down to a maximum thickness h_{MAX}, estimated from the vapour pressures, p_0, and the densities, ρ, for each species and the average weighted porosity according to $p_{AV} = (p_H d_H + p_L d_L)/(d_H + d_L) = 54\%$. In Table 1, we report the values of p_0, ρ, mass (molar content) in the vapour phase inside the flow cell before condensation, m_V (n_V), and the thicknesses, h_{MAX}, for each of the three species. In all cases, h_{MAX} is smaller than L, therefore we must expect diffusion of the liquid in the empty region after the initial condensation.

We performed numerical calculations of the maximum shift of the resonance $\Delta\lambda_{MAX,TH}$ for PS-1DPC filled with each of the three liquid species within a thickness h_{MAX} (see Table 1). In the calculations, we assumed a Bruggeman effective index approximation for the refractive indices of the layers,[20] taking into account the porosity and refractive indices of the liquids as reported in Table 1. The $\Delta\lambda_{MAX,TH}$ values are much larger than the measured ones $\Delta\lambda_{MAX,EXP}$ (Table 1), indicating that the vapour does not completely condense, as clearly expected, and that the liquid is probably not completely filling the pores. In the following, we shall therefore assume that each species condenses and uniformly fills the PS-1DPC to a thickness h_0 with a concentration of the liquid c_0. We observe that, owing to the larger p_0, m_V for methanol is larger and condensation will likely occupy a thicker layer. Such an observation justifies the unexpected inversion appearing in Fig. 3, where the sensor response to methanol is larger than that to ethanol, despite the fact that the methanol refractive index, and therefore the perturbation to the photonic structure, is smaller (see Table 1).

Diffusion can be described by the one dimensional diffusion equation:

$$\frac{\partial^2 c(x,t)}{\partial x^2} = \frac{1}{k}\frac{\partial c(x,t)}{\partial t}, \quad (1)$$

where x is the position inside the sensor measured from the surface, $c(x,t)$ is the time- and space-dependent relative concentration ($c = 1$ means pores completely filled), k is the average diffusion coefficient in the PS structure, that is assumed to be uniform along the structure and related to the average porosity, p_{AV}. We solved the eqn (1) assuming the initial conditions:

$$c(x,0) = c_0 \text{ for } 0 \le x \le h_0 \quad (2)$$

$$c(x,0) = c_0 \text{ for } h_0 < x \le L \quad (3)$$

We assume that, after the initial condensation, equilibrium between the vapour phase and the liquid in PS is reached and no further condensation can take place. Therefore no liquid can flow through the top surface of the membrane:

$$\left.\frac{\partial c(x,t)}{\partial x}\right|_{x=0} = 0 \text{ for } t>0. \quad (4)$$

We also assumed that the flow is zero at the bottom surface of the membrane, as the pores are tapped by the glass substrate with the polymeric film:

$$\left.\frac{\partial c(x,t)}{\partial x}\right|_{x=L} = 0 \text{ for } t>0. \quad (5)$$

The solution of eqn (1) is then given in the form of an infinite summation of symmetric harmonic modes:

$$c(x,t) = c_0\left[\frac{h_0}{L} + \frac{2}{\pi}\sum_{\alpha=1}^{\infty}\frac{1}{i}\sin\left(\frac{\alpha\pi h_0}{L}\right)e^{-k\left(\frac{\alpha\pi}{L}\right)^2 t}\cos\left(\frac{\alpha\pi}{L}x\right)\right], \quad (6)$$

with $\alpha \in \aleph$.

In Fig. 4, we show the normalised spatial distribution, $c(x;t_m)/c_0$, calculated by limiting the sum to the first five thousand terms, at several different times, $t_m > 0$ for $h_0 = h_{MAX}$ for ethanol. In the calculation we set $k = 6.9 \times 10^{-14}$ m^2 s^{-1}. In Fig. 4, the rapidly oscillating curve is the transverse intensity distribution of the BSW excited at $\lambda = 1480$ nm in the unperturbed PS-1DPC (in arbitrary units); making use of the figure background, showing the PS-1DPC structure, one can appreciate the region where the BSW is sensing the presence of the condensed liquid. One can clearly observe that $c(x;t_m)$ gets more and more uniform for large t_m and that the concentration at the surface is decreasing with time. Also the first moment of the distribution shifts inside the structure. These two phenomena are responsible for the decays measured and shown in Fig. 3.

Eqn (6) also shows that $c(x_0,t)$, at any point, x_0, inside the sensor, decays in a multi-exponential manner. In the inset of Fig. 3, we plot the time dependency of $c(x_0,t)$ for three fixed depths $x_0 = 0$, $x_0 = h_0$ and $x_0 = 2h_0$; the quantity, $c(x_0,t)/c_0$–h_0/L, is plotted on a logarithmic scale to show the decay characteristics. We observe that, after sufficient time, the

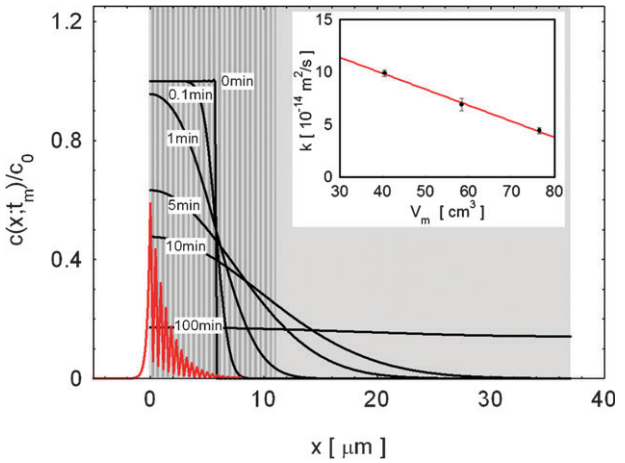

Fig. 4 Evolution of the normalized concentration $c(x;t_m)/c_0$ calculated according to the eqn (6) at several different times t_m. The figure background sketches the PS-1DPC structure for reference. The rapidly oscillating solid curve is the transverse intensity distribution of the BSW in arbitrary units. The BSW is localized at the surface, well contained in the PS-1DPC, and probes the liquid concentration mainly at the surface. Inset: plot of the diffusion coefficients obtained from the long time constant (τ_L) extracted from Fig. 3 *versus* the molecular volume for each investigated species.

decay becomes single-exponential with the same time constant regardless of the values chosen for h_0 and c_0. Such behavior is due to the fact that the decay constant of each harmonic component scales with the square of its order, α^2, and that, after sufficient time, only the lowest harmonic ($\alpha = 1$) survives with time constant $\tau_1 = k\pi^2/L^2$. This time constant appears in the measurements as τ_L. The initial steeper behavior is the contribution of the higher harmonics that depends on x_0. Comparing the experimental curves reported in Fig. 3 with those shown in the inset (long dashed curve) we have the confirmation that the experimentally observed features are due to changes taking place at the surface of the sensor.

Therefore, regardless of the knowledge of h_0, c_0 and of the fast dynamics, and assuming that $\tau_L = \tau_1 = k\pi^2/L^2$, we can finally extract the diffusion coefficients from the experimental values for all the investigated species inside the PS-1DPC, obtaining the experimental values for k reported in Table 1. In the inset of Fig. 4 we plot the estimated k as a function of the molecular volume V_m. In the limited range of molecular volumes probed during the experiments the k values scale linearly with V_m. Such result is in agreement with observations by Motohashi *et al.* who showed that the peak frequency of the dielectric loss angle of vapour molecules in PS gas sensors scales linearly with V_m too.[21]

In conclusion, we have demonstrated that it is possible to fabricate very fast gas sensors based on Bloch surface waves propagating at the truncation surface of a porous silicon one-dimensional photonic crystal. A new configuration, involving the use of free standing membranes bound to transparent substrates, allows excitation of the surface waves and sensing of the associated perturbation upon exposure to organic vapours, reaching an unprecedented response time, smaller than the experimental resolution of our setup, that is in the order of 30 s. If a single wavelength sensing scheme is used, the response time could be further decreased. Moreover, diffusion of the liquids condensed inside the porous silicon sensors gives rise to a long term decay of the response bearing the signature of the specific vapour. We showed that the three vapours used in the experiments are characterized by different long term time constants, and diffusion coefficients which are well described by a model in which the diffusion constant is proportional to the molecular volume. The measurement of the long term decay constant for an unknown gas and comparison to calibration values can lead to selective sensing. Further characterization of the sensitivity, reproducibility and selectivity in the presence of an interfering gas and a comparison with other/conventional vapour sensor systems in terms of such parameters is needed. Being aware that such issues are fundamental for the realization of a reliable sensor, they are the subject of our future applied research.

Acknowledgements

This work is supported by two Piedmont Regional projects CIPE 2008 "Photonic biosensors for early cancer diagnostics (PHOENICS)" and "Nanomaterials and technologies for intelligent monitoring of quality, safety and traceability in confectionery products" (NAMATECH), by the Fondo Integrativo per la Ricerca di Base 2004 Laboratorio di Tecnologie Elettrobiochimiche Miniaturizzate per l'Analisi e la Ricerca (LATEMAR) and by the Science and Technology Atheneum Research Programme of the SAPIENZA University.

References

1 R. C. Anderson, R. S. Muller and C. W. Tobias, *Sens. Actuators, A*, 1990, **23**, 835.
2 S. Zangooie, R. Bjorklund and H. Arwin, *Sens. Actuators, B*, 1997, **43**, 168.
3 C. L. Curtis, V. V. Doan, G. M. Credo and M. J. Sailor, *J. Electrochem. Soc.*, 1993, **140**, 3492; J. Gao, T. Gao and M. J. Sailor, *Appl. Phys. Lett.*, 2000, **77**, 901.
4 P. A. Snow, E. K. Squire, P. St. J. Russell and L. T. Canham, *J. Appl. Phys.*, 1999, **86**, 1781.
5 V. Mulloni and L. Pavesi, *Appl. Phys. Lett.*, 2000, **76**, 2523.
6 B. Sciacca, F. Frascella, A. Venturello, P. Rivolo, E. Descrovi, F. Giorgis and F. Geobaldo, *Sens. Actuators, B*, 2009, **137**, 467.
7 M. Ghulinyan, Z. Gaburro, D. S. Wiersma and L. Pavesi, *Phys. Rev. B: Condens. Matter Mater. Phys.*, 2006, **74**, 045118.
8 E. Guillermain, V. Lysenko, R. Orobtchouk, T. Benyattou, S. Roux, A. Pillonnet and P. Perriat, *Appl. Phys. Lett.*, 2007, **90**, 241116.
9 P. Yeh, A. Yariv and C.-S. Hong, *J. Opt. Soc. Am.*, 1977, **67**, 423.
10 W. M. Robertson and M. S. May, *Appl. Phys. Lett.*, 1999, **74**, 1800.
11 E. Descrovi, T. Sfez, L. Dominici, W. Nakagawa, F. Michelotti, F. Giorgis and H.-P. Herzig, *Opt. Express*, 2008, **16**, 5453.
12 M. Liscidini and J. E. Sipe, *J. Opt. Soc. Am. B*, 2009, **26**(2), 279.
13 M. Shinn and W. M. Robertson, *Sens. Actuators, B*, 2005, **105**, 360.
14 E. Descrovi, F. Frascella, B. Sciacca, F. Geobaldo, L. Dominici and F. Michelotti, *Appl. Phys. Lett.*, 2007, **91**, 241109.
15 F. Geobaldo, P. Rivolo, S. Borini, L. Boarino, G. Amato, M. Chiesa and E. Garrone, *J. Phys. Chem. B*, 2004, **108**, 18306.
16 E. Descrovi, F. Giorgis, L. Dominici and F. Michelotti, *Opt. Lett.*, 2008, **33**, 243.
17 A. S. Ramírez-Duverger, J. Gaspar-Armenta and Raúl García-Llamas, *Opt. Commun.*, 2007, **277**, 302.
18 R. Ulrich, *J. Opt. Soc. Am.*, 1970, **60**, 1337.
19 Z. Gaburro, N. Daldosso, L. Pavesi, G. Faglia, C. Baratto and G. Sberveglieri, *Appl. Phys. Lett.*, 2001, **78**, 3744.
20 D. A. G. Bruggemann, *Ann. Phys.*, 1935, **416**, 636.
21 A. Motohashi, M. Kawakami, H. Aoyagi, A. Kinoshita and A. Satou, *Jpn. J. Appl. Phys.*, 1995, **34**, 5840.

